interpenetration of hydration shells. This interpenetration results in the loss of one of the strong hydrogen bonds of the H_9O_4 unit.[23] This transition state is also consistent with the observation of a small, inverse, isotope effect, between 0.67 and 0.77, when BD_4^- is substituted for BH_4^-,[24] because the binding of the BH_4^- anion to its neighbors in solution is being strengthened, while no B–H bond is being broken. Hammes[25] has found a mechanism related to this in which the rate-determining step of the dimerization of 2-pyridone in DMSO mixtures is the dissociation of the dimethyl sulfoxide–2-pyridone hydrogen bond.

It is interesting to note that the magnitude of k_H (10^6 M^{-1} sec^{-1})[13] leads to a free energy of activation of 9.3 kcal mol^{-1}. The standard free energy of bringing together the reagents for an acid-catalyzed proton transfer to carbon, and appropriately resolvating them, W^r, has been recently estimated as about 8 kcal mol^{-1}, using Marcus' formulation.[26] The correspondence is just about what might be expected if we are, here, measuring the rate of a similar process for which W^r is the standard free energy.

The reprotonations of β-diketone anions[27,28] and cyanocarbon anions[29,30] have rate constants similar to those discussed here and may well use analogous mechanisms.

(23) R. A. More O'Ferrall, G. W. Koeppl, and A. J. Kresge, *J. Amer. Chem. Soc.*, **93**, 1 (1971).
(24) R. E. Davis and C. L. Kibby, *ibid.*, **82**, 5950 (1960).
(25) G. G. Hammes and P. J. Gillford, *ibid.*, **92**, 7578 (1970).
(26) M. M. Kreevoy and D. E. Konasewich, *Advan. Chem. Phys.*, **21**, 243 (1971).
(27) T. Riley and F. A. Long, *J. Amer. Chem. Soc.*, **84**, 522 (1962).
(28) F. A. Long and D. Watson, *ibid.*, **80**, 2019 (1958).
(29) F. Hibbert and F. A. Long, *ibid.*, **93**, 2826 (1971).
(30) F. Hibbert, F. A. Long, and E. A. Walters, *ibid.*, **93**, 2829 (1971)

Infrared and Raman Spectra of Gaseous and Matrix Isolated Beryllium Borohydride

Joseph W. Nibler

Contribution from the Department of Chemistry, Oregon State University, Corvallis, Oregon 97331. *Received September 3, 1971*

Abstract: Infrared spectra of gaseous and matrix isolated beryllium borohydride (BeB_2H_8, BeB_2D_8, and BeB_2HD_7) are presented. In addition Raman spectra have been recorded for the gas despite the low vapor pressure of ~10 mm and, in one of its first applications, Raman matrix isolation spectra were obtained. Depolarization measurements were made for both the gas and the matrix. The results indicate that two distinct structures of BeB_2H_8 coexist in equilibrium in the vapor phase. On cooling to 20°K *via* the matrix, the equilibrium shifts and only one form is trapped. Isotopic data and the Raman depolarization results are most consistent with a C_{3v} configuration which is obtained by distorting a D_{3d} structure so as to produce a double minimum for the Be atom. A frequency assignment is presented for this C_{3v} model and a brief discussion of the unusual bonding about the Be atom is given. The frequencies corresponding to the second form of gaseous BeB_2H_8 suggest the presence of a terminal BH_2 group and a double hydrogen bridge but do not allow a clear distinction between the classical D_{2d} structure and a triangular configuration.

The structure of gaseous beryllium borohydride, BeB_2H_8, continues to be a subject of some controversy. To date, no fewer than five different configurations (I–V in Figure 1) have been proposed, yet none can be viewed as established. Because of its volatility, BeB_2H_8 is classed as a covalent borohydride such as $Al(BH_4)_3$ and $Zr(BH_4)_4$. It was first prepared[1] in 1940 by the reaction of B_2H_6 and $Be(CH_3)_2$ and, from vapor density measurements, was found to exist as monomeric BeB_2H_8. In 1946 an electron diffraction experiment[2] was interpreted in terms of a triple hydrogen bridged D_{3d} model I but shortly thereafter, from an infrared study, Longuet-Higgins[3] suggested that a double bridged D_{2d} structure II was more reasonable. Reexamination[4] of the original electron diffraction data showed that such a model could be accommodated if the bridge bonds were highly asymmetrical.

Thus the D_{2d} structure was considered to be established until 1967 when the Oslo electron diffraction group repeated the experiment[5] and, surprisingly, found that their new data were not compatible with II but were consistent with a triangular C_{2v} structure III. Shortly thereafter mass spectroscopic and infrared results were reported[6] to favor a singly bridged triangular structure IV of C_2 symmetry. About the same time, we noted[7] that the vapor infrared vibration–rotation band contours were not those of a rigid rotor symmetric top (II) but were more consistent with III (or IV). We also reported a dipole moment of 2.1 ± 0.5 D from dielectric measurements. The existence of a substantial dipole moment was later confirmed by an electric deflection experiment.[8] However, it should be noted that several attempts[9] to obtain a microwave spectrum

(1) A. Burg and H. I. Schlesinger, *J. Amer. Chem. Soc.*, **62**, 3425 (1940).
(2) G. Silbiger and S. H. Bauer, *ibid.*, **68**, 312 (1946).
(3) H. C. Longuet-Higgins, *J. Chem. Soc.*, 139 (1946).
(4) S. H. Bauer, *J. Amer. Chem. Soc.*, 72, 622 (1950).
(5) A. Almenningen, G. Gundersen, and A. Haaland, *Acta Chem. Scand.*, **22**, 859 (1968).
(6) T. H. Cook and G. L. Morgan, *J. Amer. Chem. Soc.*, **91**, 774 (1969).
(7) J. W. Nibler and J. McNabb, *Chem. Commun.*, 134 (1969).
(8) J. W. Nibler and T. Dyke, *J. Amer. Chem. Soc.*, **92**, 2920 (1970).

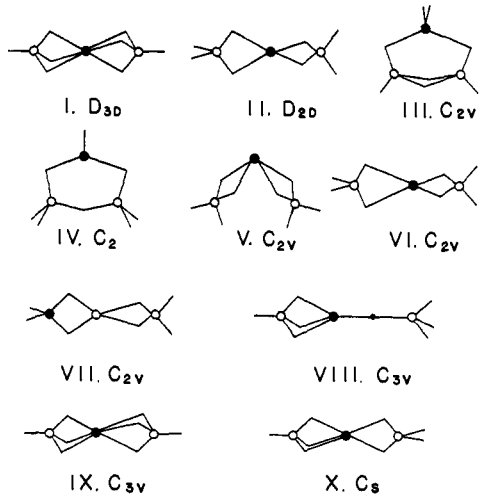

Figure 1. Various possible structures for BeB_2H_8.

were unsuccessful, presumably because of decomposition on the metal cavity surfaces. An effort to do the microwave experiment in a Teflon-coated cavity is under way.[10]

Because structure III (or IV) represented such a complete change from the earlier models I and II, the electron diffraction experiment has recently been repeated both at Oslo and at Oregon State. The Oslo data are incomplete, but the diffraction pattern is clearly similar to the pattern obtained at Oregon State. Quite remarkably, however, the radial distribution curve obtained from analysis of the O. S. U. data *does not agree* closely with either the 1946 or the 1967 curves. Efforts to fit this data to models II–V have not been successful. However, a D_{3d} structure I and a C_{3v} structure IX were found to give good fits albeit with bond lengths which differ considerably from those of the 1946 model. This work will be discussed by Gundersen and Hedberg in a separate publication.[11]

Very recently, an X-ray diffraction study[12] by Marynick and Lipscomb has determined that the solid exists as a helical chain of the sort

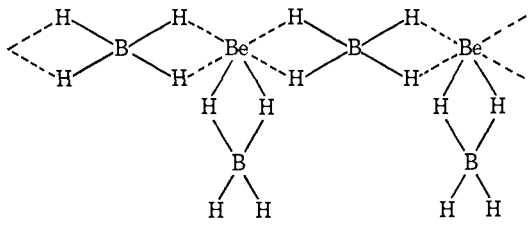

Although the hydrogens could not be precisely placed, the unusual "octahedron" of hydrogens around Be was shown to be considerably distorted. In general, the structure is in reasonable accord with our earlier conclusion[13] from infrared and Raman studies that the solid consists of coupled $H_2BH_2Be^+$, BH_4^- ions. This borderline tendency of BeB_2H_8 toward an ionic structure is consistent with the fact that all other group II (and group I) borohydrides are ionic salts. Unfortunately, the solid structure offers no direct aid in deducing the vapor structure since spectral changes on vaporization imply significant structural changes.

Concurrent with our investigation, Cook and Morgan[14] have done a detailed infrared study of vapor phase BeB_2H_8, BeB_2D_8, and $Be^{10}B_2D_8$ down to 400 cm^{-1}. They interpret their data in terms of a new C_{2v} structure V. They also infer the presence of dimers in the vapor from intensity changes with pressure. Although our vapor spectra are generally similar to theirs, our results differ in several important respects. (a) We have repeated the vapor density experiment at 5 mm and 27° and find no evidence for dimers. This is in accord with Burg and Schlesingers' measurements[1] and in fact with Cook and Morgans' earlier interpretation[6] of the mass spectrum of BeB_2H_8. (b) We have not been able to reproduce their pressure dependent spectral changes. (c) The rotational fine structure which they observe in the terminal BH stretching region is due to B_2H_6 impurity, not BeB_2H_8. We have been able to eliminate such structure both by compensation with B_2H_6 in the reference beam and by careful distillation. Detailed examination of pure BeB_2H_8 under high-resolution conditions (0.3 cm^{-1} on a Perkin-Elmer 180) reveals no rotational structure. (Such structure is easily resolved for B_2H_6.) (d) We offer a different interpretation of the rotational band contours upon which their C_{2v} structure is partially based.

We present here infrared and Raman spectra of gaseous and matrix isolated BeB_2H_8 and BeB_2D_8. The Raman spectra merit special attention since the vapor spectra were obtained at unusually low pressures (~10 mm) and the matrix spectra represent one of the first applications of Raman matrix isolation spectroscopy to a system of chemical interest. The results reveal several new features of this problem and suggest a possible explanation of the different experimental results.

Experimental Section

Following the method of Schlesinger, *et al.*,[15] beryllium borohydride was sublimed from a powdered mixture of anhydrous $BeCl_2$ and $LiBH_4$ (both 97+% Alfa Inorganics, Inc.) or $LiBD_4$ (>95% Fluka A.G.). Because of its poisonous, flammable nature, all handling of BeB_2H_8 was done in a hood using a vacuum line greased with Kel F. Samples were distilled before each experiment to eliminate traces of B_2H_6 which slowly form as a decomposition product.

The vapor density measurement was performed at 27° using an inert oil (Halocarbon Products Corp., series 10-25) manometer. BeB_2H_8 (32.7 mg) expanded into a volume of 3.55 l. produced an unsaturated pressure of 4.92 Torr, giving M = 37.1 g/mol. At −78°, 31.3 mg was recollected and, allowing for noncondensed sample (pressure after 1 hr was 0.17 mm), a check value of 36.8 g/mol was obtained. The calculated value for BeB_2H_8 is 38.7 g/mol. The differences are about the same as our experimental uncertainty. These results plus earlier determinations by Burg and Schlesinger[1] (38.0, 38.5, and 39.0 g/mol) indicate that very little, if any, dimer is present.

Because of the reaction of BeB_2H_8 with NaCl and KBr infrared gas cell windows,[16] special care was taken to minimize window bands. At various times, IR-TRAN 2, LiF, BaF_2, and CsI windows were used. All reacted slightly with BeB_2H_8 but the infrared absorptions were weak and easily identified since they persisted upon pumping out the cell. Window absorptions were stronger for

(9) Private communication: H. Møllendal, University of Oslo; D. Levy, University of Chicago.
(10) Private communication: R. D. Brown, Monash University.
(11) G. Gundersen and K. W. Hedberg, to be published.
(12) D. S. Marynick and W. N. Lipscomb, *J. Amer. Chem. Soc.*, **93**, 2322 (1971).
(13) J. W. Nibler, D. F. Shriver, and T. H. Cook, *J. Chem. Phys.*, **54**, 5257 (1971).
(14) T. H. Cook and G. L. Morgan, *J. Amer. Chem. Soc.*, **92**, 6493 (1971).
(15) H. I. Schlesinger, H. C. Brown, and E. K. Hyde, *ibid.*, **75**, 209 (1953).
(16) W. C. Price, *J. Chem. Phys.*, **17**, 1044 (1949).

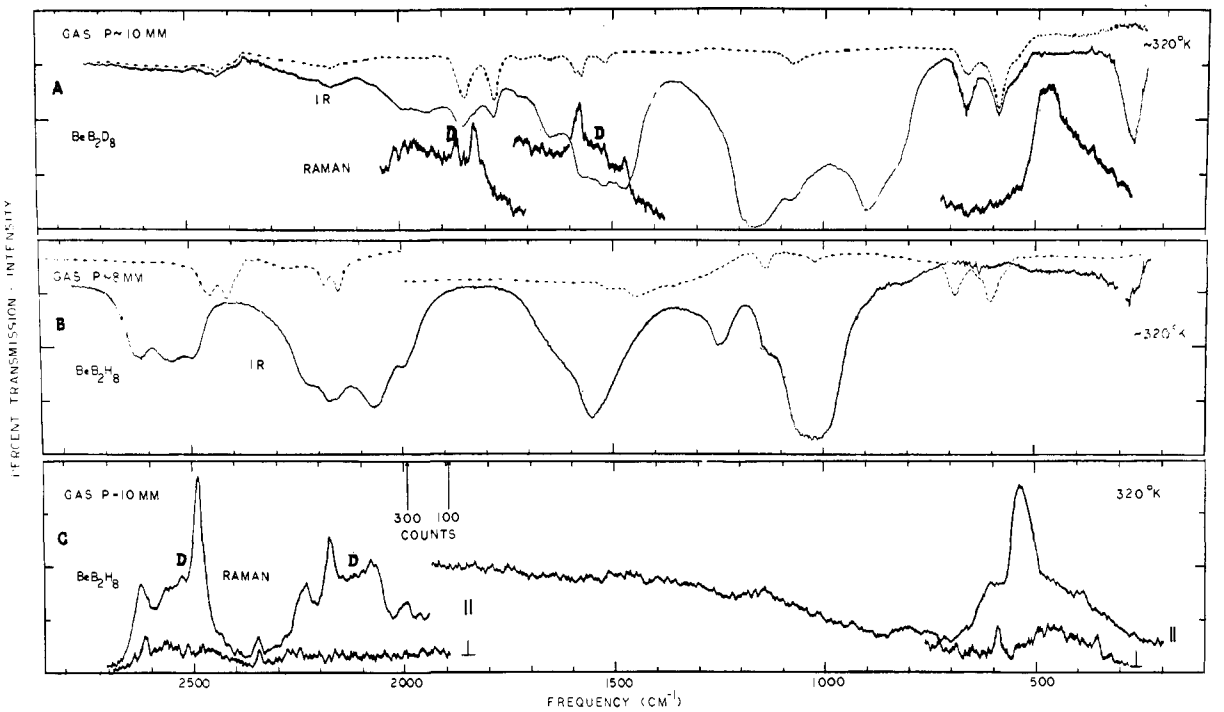

Figure 2. Infrared and Raman spectra of gaseous beryllium borohydride. A, BeB_2D_8 (-----) empty 10-cm cell (CsI windows) after evacuation of BeB_2D_8; (——) infrared spectrum; (——) Raman spectrum (D = diborane). B, BeB_2H_8 (-----) empty 10-cm cell (CsI windows) after evacuation of BeB_2H_8; (——) infrared spectrum. C, BeB_2H_8, Raman depolarization spectra.

BeB_2D_8 than BeB_2H_8, perhaps in keeping with the lower volatility of the deuteride. A Beckman IR-7 with CsI interchange was used to cover the infrared region from 4000 to 225 cm^{-1} with a resolution of 2 cm^{-1} or better. A Perkin-Elmer 180 was used for the high-resolution gas-phase studies.

The vapor-phase Raman spectra were obtained with a Cary 82 spectrophotometer and a Coherent Radiation 52B argon ion laser operated at 5145 Å at a power level of 800 mW at the sample. A quartz multiple reflection cell was used to give an increase of ~10 in the Raman signal. Because the vapor pressure of BeB_2H_8 is only 10 mm at room temperature, spectral slit widths varying from 5 to 10 cm^{-1} were used. In some experiments the cell was heated to 45° to increase the vapor pressure to ~40 mm. Spectra were obtained both with and without solid present with no apparent difference. However, traces of diborane were observed and, in one run, also an unknown boron hydride with features at 2570 (m, p), 815 (vw), 760 (w, p), 588 (s, dp), and 357 cm^{-1} (w).

The infrared matrix experiments were done at 15–20°K using a CsI window cooled by an Air Products AC-3L cryotip with a conventional dewar of our design. The Raman matrix experiments were done at 12–14°K using an Air Products Displex refrigerator. The experimental techniques for Raman matrix isolation spectroscopy will be described separately.[17] Argon and nitrogen (99.999%, Matheson) were used at matrix ratios of 150–1000. Most experiments were done at relatively low matrix ratios of 150–300 because of problems of decomposition with time. A short glass spray on line and a stainless steel needle valve were used to minimize the decomposition, but some diborane always appeared along with a white solid residue (probably polymeric $BeBH_5$ and/or BeH_2). Most of the solid formed on the walls of the sample gas bulb, although traces may have made it to the cold tip in some experiments. BeB_2D_8 seemed less stable than BeB_2H_8 and decomposition was particularly troublesome in the Raman experiments because of the long, slow spray on rates required for glassy matrices.

Results and Discussion

Vapor Spectra. Infrared and Raman spectra of gaseous BeB_2H_8 and BeB_2D_8 are presented in Figure 2 and the frequencies are tabulated in Tables I and II. Because the bands are broad and heavily overlapped, most of the tabulated frequencies have a large uncertainty (~2–10 cm^{-1}). For reference, Table III

Table I. Infrared and Raman Frequencies (cm^{-1}) of BeB_2H_8[a]

Gas		Argon matrix	
Ir	Raman	Ir	Raman
			2714 vw
2624 m	2627 m, p	2645 m	2643 s, p
	2616 w		
2550 m	~2550 m	2565 vw	2566 vw
2500 m	2490 s, p	2505 w	
		2391 vw	
	2352 w, dp	2347 vw, ?	
	2240 m, p		2255 s, p
2225 m, sh		2241 s	2235 w, sh
		2202 vs	
2167 s	2175 s, p	2172 m	2179 s, p
2071 s	2075 m, p	2066 vw	
2000 w, sh	1995 w, p	1995 vw	2010 vw
~1650 m, sh		1658 vw	1615 vw, dp
1548 s, b		1560 vw	
		1510 w, ?	
		1475 vw	
		1284 w	1298 w, dp
1247 w		1245 s	
		1205 vw, ?	
		1184 vvw	1184 vw
1130 w, sh	~1150 vw, b	1123 m	1105 s, p, ?
~1050 vs, b		1051 vs	
~1000 vs, b			1002 vw, p
		904 vw, ?	
		770 vw	775 vw, p
		743 vvw	740 vw, dp
		665 vw	668 m, p
			635 m, p
	588 w, dp, ?	595 w, b	588 m, p, ?
	535 s, b, p		540 m, p
			445 m, dp
	384 vw	386 vw	390 vw, dp
		368 vw	
	357 vw	355 vw	
287 w		280 vs	290 vw, dp

[a] Features with ? vary randomly in relative intensity.

(17) J. W. Nibler and D. Coe, *J. Chem. Phys.*, **55**, 5133 (1971).

Table II. Infrared and Raman Frequencies (cm^{-1}) of BeB_2D_8[a]

Gas		Argon matrix	
Ir	Raman	Ir	Raman
~2650–		2626 vw	
2450 vw, b			
~2300–		2251 w	
2100 vw, b		2178 w	
2000 w		2003 w	
1935 w		1925 w, ?	
		1838 w, ?	
1820 w	1826 s, p	1829 vw	
1650 m, sh		1647 vs	1617 m, dp, ?
		1595 w, sh	1597 m, sh, p
1580 s, b	1578 s, p	1577 vs	1583 s, p
~1520 s, b	1520 m	1545 vw, ?	
		1492 vw, ?	
1470 s	1471 m, p	1470 vw	
		1456 vw, sh	
		1262 vvw	
		1245 vvw	1230 w
1166 vs, b		1153 vw, ?	
		1118 m, ?	1115 w, b, p
1075 w, sh		1074 s	1033 w, p
			1002 m, p
960 vw, sh		928 vw, sh	940 vw
895 vs, b		893 vvs	
830 s, sh			
		747 vw	
		714 vw	
665 w		654 vvw	669 m, p
		630 w	635 w, p
		563 vw	556 vvw
		543 vw	
		494 w, b	500 w, p
	478 s, p		471 w
			443 m, p
			391 w
		322 m	335 vw
		302 m	292 vw, dp
275 m		253 vs	261 vw, dp

[a] Features with ? vary randomly in relative intensity.

summarizes the group theoretical predictions for the vibrations of various models of BeB_2H_8. These classifications by approximate mode type and expected frequency region are, of course, only rough estimates but they do help in interpreting the spectra. In particular, localized modes such as the terminal and bridged BH stretches and the low frequency skeletal modes can be assigned with reasonable confidence. The prediction of the number and types of polarized Raman vibrations is also of great value in the analysis.

Before discussing the vapor spectra in detail, it is necessary to consider the possibility that some of the peaks in Figure 2 may represent partially resolved rotational band contours. Morgan and Cook[14] have in fact assumed this and base their structure V in part on their calculated values of P–R branch separation ($\Delta\nu$) for the symmetric BH stretch of models II and V. They obtain 18.1 cm^{-1} for $\Delta\nu$ for model II (method of Gerhard and Dennison[18]) *vs.* 35.4 cm^{-1} for model V (method of Badger and Zumwalt[19]). Unfortunately, the experimental $\Delta\nu$ (41 cm^{-1} centered around a Q branch at 2521 cm^{-1}) that they cite as favoring V is surely incorrect because this Q branch is that of B_2H_6 impurity. Moreover, we prefer to view most of the major features as unresolved P, Q, and R branches of independent fundamentals for the following reasons.

First, there is a striking coincidence between the infrared and Raman spectra above 2000 cm^{-1}. Normally only totally symmetric modes have high Raman intensity and since for these only the Q branch is intense, this strongly indicates that all the main features are vibrational fundamentals (gas-phase Raman spectra of B_2H_6 show only a sharp Q branch for each symmetric vibration[20]).

Second, all perpendicular bands for a linear skeleton should be broad and Gaussian in shape with no rotational contours. This statement is based on the limiting Gaussian expression of Gerhard and Dennison[18] for the band shape of perpendicular modes of extreme ($A/B \gtrsim 5$) prolate tops (for linear BeB_2H_8, $A/B \sim 10$–11).

Finally, if the heavy atoms form a linear skeleton, as seems required by the latest electron diffraction results, the molecule is exactly (models I, II, VIII, IX) or nearly exactly (models VI, VII, X) a prolate symmetric top. Thus in the rigid rotor approximation one might expect distinct PQR structure for the parallel modes, with a P–R separation of the order of 18 cm^{-1}. In an earlier note, we in fact cited the absence of such rotational structure as being consistent with a nonlinear skeleton. However, we now feel that it is more likely that such structure is simply unresolved due to (a) overlap of the features of $Be^{11}B_2H_8$ (65%), $Be^{10}B^{11}BH_8$ (31%), and $Be^{10}B_2H_8$ (4%); (b) a complex pattern of rotational lines because of significant differences between the rotational constants in the ground and excited vibrational levels (this is consistant with a "floppy" sort of structure and with the relatively broad Q branches observed in the Raman spectra); (c) blurring by transitions originating from vibrationally excited molecules with slightly different rotational constants (indeed, the observation of a skeletal bending mode at 287 cm^{-1} implies that 27% of the molecules are vibrationally excited in this mode alone at 320°K); (d) decrease in the Q branch intensity relative to the P and R branches (using the method of Gerhard and Dennison,[18] a factor of 2 reduction for this intensity ratio is calculated in going from B_2H_6 to linear BeB_2H_8); (e) overlap of bands due to the possible existence of several forms of BeB_2H_8 (see later).

If one considers a bent structure, the molecule is an asymmetric top and the prediction of band contours from the approximate calculations of Badger and Zumwalt can lead to erroneous interpretations.[21] Ueda and Shimanouchi[21] have improved on these calculations and they present 40 figures giving the calculated band contours of various asymmetric tops. Comparison of the observed spectra with their figures (22, 13) most appropriate for the rotational constants of models III and V (and probably any significantly bent model) shows no similarity. Thus the rotational contours are most consistent with a linear skeleton or, possibly, with the overlapping bands of several structures.

Matrix Spectra. Infrared and Raman spectra of matrix isolated BeB_2H_8 and BeB_2D_8 are presented in Figures 3 and 4 and the frequencies are tabulated in Tables I and II. All matrix spectra contain diborane peaks (dashed lines) due to decomposition during the lengthy spray on periods. Comparison with the gas-phase spectra in Figure 2 reveals a number of

(18) S. L. Gerhard and D. M. Dennison, *Phys. Rev.*, **43**, 197 (1935).
(19) R. M. Badger and L. R. Zumwalt, *J. Chem. Phys.*, **6**, 711 (1938).
(20) R. V. Taylor and A. R. Emery, *Spectrochim. Acta*, **10**, 419 (1958).
(21) T. Ueda and T. Shimanouchi, *J. Mol. Spectrosc.*, **28**, 350 (1968).

Table III. Vibrational Modes for Various Models of BeB_2H_8

Model	Symmetry species and activity	Approximate mode types and expected frequency regions: ν BH_t, 2350–2650	ν BeH_t (1700–2350?)	ν BH_b, 1500–2200	ν BeH_b or δ BH_{2b} (1000–2000?)	δ, ρ_r, ρ_w BH_{t2}, BeH_{t2}, 900–1250	δ BH_t, BeH_t, 900–1200	Torsion, 600–1000	ν BBe, 500–1100	Ring bends, 300–500	δ BBeB, 200–300	Summary[a]
I (D_{3d})	A_{1g} (R, p)	1		1	1		0	0	1	0	0	Ir = 9
	E_g (R)	0		1	1		1	0	0	1	0	R = 4p + 4dp
	A_{1u}	0		0	0		0	1	0	0	0	C = 0
	A_{2u} (ir)	1		1	1		0	0	1	0	0	
	E_u (ir)	0		1	1		1	0	0	1	1	
II (D_{2d})	A_1 (R, p)	1		1	1	1		0	1	0	0	Ir = 12
	A_2	0		0	0	0		1	0	0	0	R = 5p + 14dp
	B_1 (R)	0		0	0	0		2	0	0	0	C = 12
	B_2 (ir, R)	1		1	1	1		0	1	0	0	
	E (ir, R)	1		1	1	2		0	0	1	1	
III (C_{2v})	A_1 (ir, R, p)	1	1	2	1	1	1	0	1	1	1	Ir = 23
	A_2 (R)	0	0	1	0	0	1	2	0	0	0	R = 10p + 17dp
	B_1 (ir, R)	1	0	2	1	1	1	0	0	2	0	C = 23
	B_2 (ir, R)	0	1	1	0	1	1	0	1	1	0	
IV (C_2)	A (ir, R, p)	2	1	2	1	3	0	1	1	1	1	Ir = 27
	B (ir, R)	2	0	2	1	3	2	0	1	3	0	R = 13p + 14dp
												C = 27
V (C_{2v})	A_1 (ir, R, p)	2		1	1	2		0	1	1	1	Ir = 22
	A_2 (R)	0		1	1	1		2	0	0	0	R = 9p + 18dp
	B_1 (ir, R)	0		1	1	1		1	0	1	0	C = 22
	B_2 (ir, R)	2		1	1	2		0	1	1	0	
VI (C_{2v})	A_1 (ir, R, p)	2		2	2	2		0	2	0	0	Ir = 24
	A_2 (R)	0		0	0	0		3	0	0	0	R = 10p + 17dp
	B_1 (ir, R)	1		1	1	2		0	0	1	1	C = 24
	B_2 (ir, R)	1		1	1	2		0	0	1	1	
VII (C_{2v})	A_1 (ir, R, p)	1	1	3	1	2		0	2	0	0	Ir = 24
	A_2 (R)	0	0	0	0	0		3	0	0	0	R = 10p + 17dp
	B_1 (ir, R)	0	1	2	0	2		0	0	1	1	C = 24
	B_2 (ir, R)	1	0	1	1	2		0	0	1	1	
VIII (C_{3v})	A_1 (ir, R, p)	2		2	1	1	0	0	2	0	0	Ir = 17
	A_2	0		0	0	0	0	1	0	0	0	R = 8p + 9dp
	E (ir, R)	1		1	1	2	1	0	0	2	1	C = 17
IX (C_{3v})	A_1 (ir, R, p)	2		2	2	1	0	0	2	0	0	Ir = 17
	A_2	0		0	0	0	0	1	0	0	0	R = 8p + 9dp
	E (ir, R)	0		2	2	2	1	0	0	2	1	C = 17
X (C_s)	A′ (ir, R, p)	3		3	3	2	1	0	2	2	1	Ir = 27
	A″(ir, R)	0		2	2	1	1	2	0	1	1	R = 17p + 10dp
												C = 27

[a] C = coincidences.

striking changes. In particular, gas-phase infrared bands at 2550, 2071, 2000, 1650, 1548, and ~1000 cm^{-1} and Raman bands at 2490, 2075, and 1995 cm^{-1} are drastically reduced in intensity in the matrix. Parallel behavior occurs for BeB_2D_8 for infrared bands at 1935, ~1550, 1470, 1166, and 830 cm^{-1} and for Raman bands at 1826 and 1471 cm^{-1}. Because such behavior is unusual and undoubtedly bears on the structure of BeB_2H_8, we list below possible explanations along with experiments we have done to test them.

(a) Dimerization: not likely since the vapor is monomeric and matrix dilution studies over a range of 150–1000 show no marked intensity changes in the major peaks. Altogether, ten infrared experiments were run on BeB_2H_8, four on BeB_2D_8, and the relative intensities of the major peaks did not vary significantly. A few of the weaker features did seem to vary slightly and these are identified with a ? in Tables I and II. Such variations could be due to decomposition fragments ($BeBH_5$, $(BeH_2)_n\cdots$) or possibly to aggregates. The spectra in Figure 4A illustrate the most marked changes observed, the lower trace showing a number of additional features apparently due to the increased spray on rate. Although their assignment as aggregate absorptions seems reasonable, they do not correlate well with the pure solid spectrum.[13] Because of the complexity of the spectrum and the instability and troublesome nature of the compound, an extensive study of aggregate bands was not undertaken.

(b) Hot bands: not likely since no logical combination-difference pairs are observed. The almost complete loss of the very intense 1548-cm^{-1} absorption is completely inconsistent with this possibility. Moreover, the observation of some small residual intensity for most features at 20°K would require thermal population of a vibrational state below 100 cm^{-1}, whereas the absence of any marked intensity changes when the matrix is warmed from 16 to 30°K argues against this.

(c) Matrix orientation: eliminated by the absence of any relative intensity changes upon rotation of the matrix film by 45°.

(d) Structural changes induced by temperature reduction and/or the matrix: possible but not favored because of the close gas-matrix frequency correspondence for all features. Also, no abnormal matrix shifts are observed in going from argon to nitrogen.

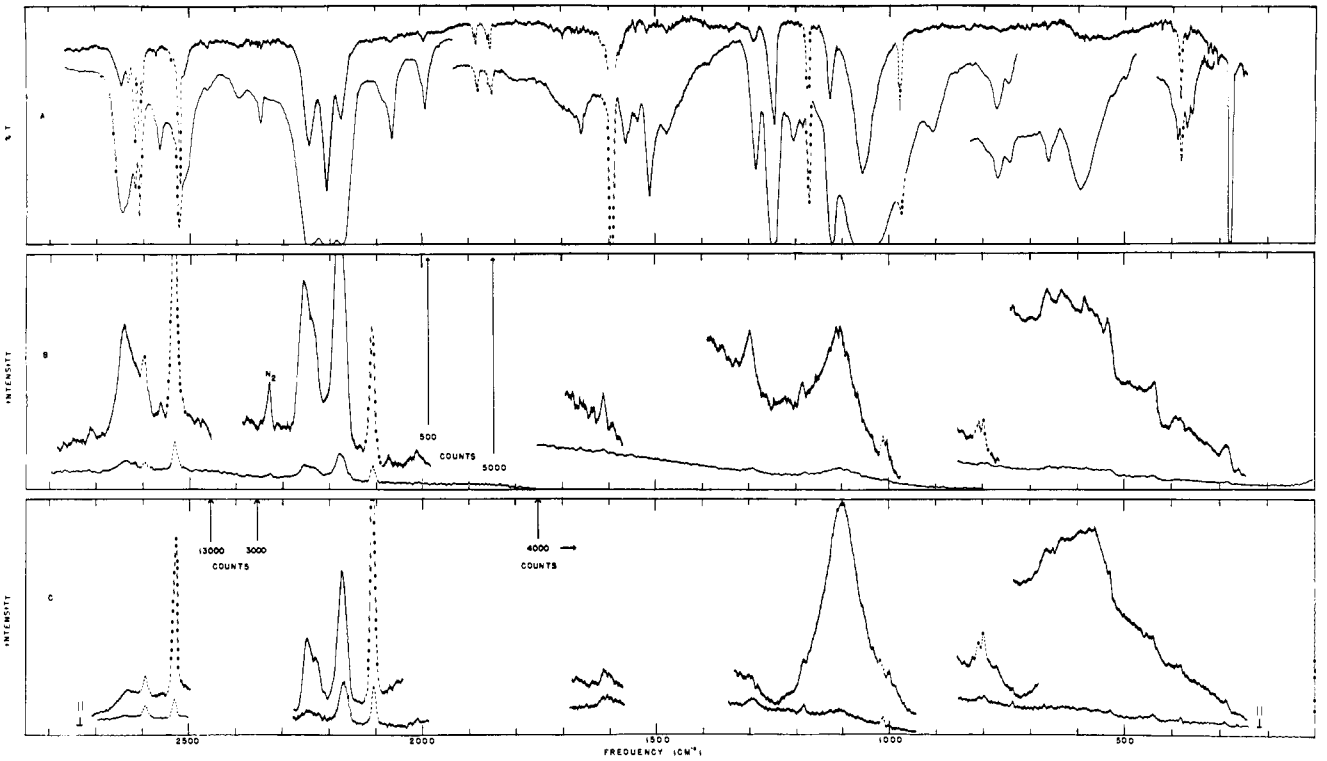

Figure 3. Infrared and Raman spectra of matrix isolated BeB_2H_8. A, infrared spectrum (20°K), upper trace = 5 mmol BeB_2H_8/Ar = 1/300 deposited in 3 hr; lower trace = 30 mmol BeB_2H_8/Ar = 1/200 deposited in 3 hr; (----------) peaks due to B_2H_6. B, Raman spectrum (14°K), 35 mmol BeB_2H_8/Ar = 1/150 deposited in 10 hr; 500 mW 4880 at sample, 4 cm^{-1} S.B.W. C, Raman spectrum (14°K), depolarization experiment, 80 mmol BeB_2H_8/Ar = 1/150 deposited in 30 hr; 500 mW 4880 at sample, 5 cm^{-1} S.B.W.

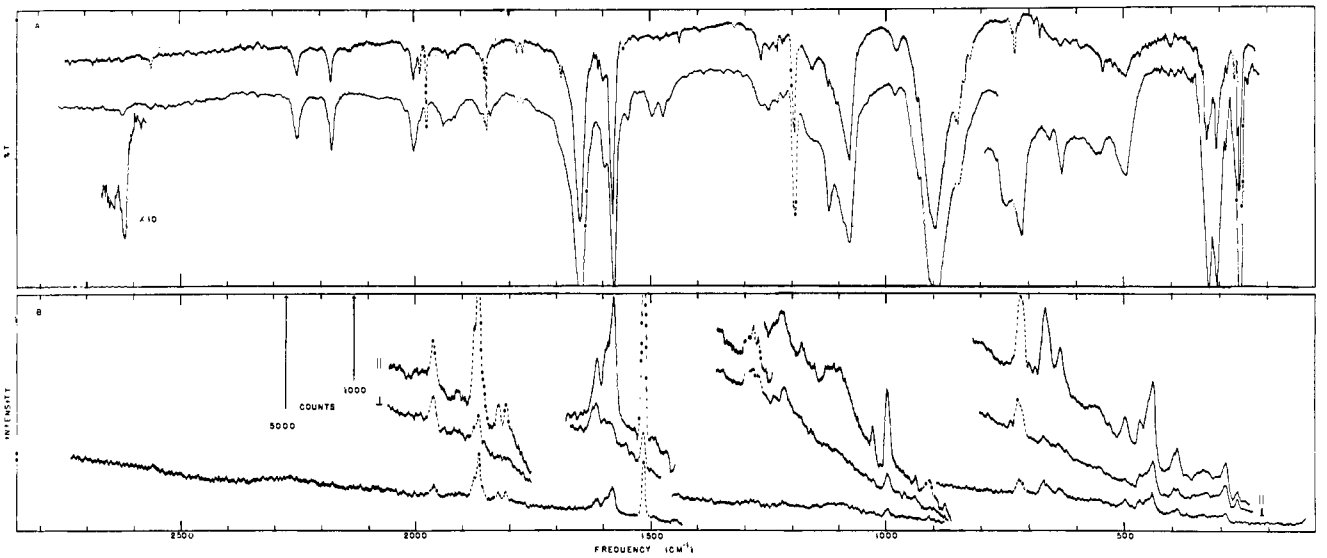

Figure 4. Infrared and Raman spectra of matrix isolated BeB_2D_8. A, infrared spectrum (20°K), upper trace = 17 mmol BeB_2D_8/Ar = 1/290 deposited in 7 hr; lower trace above 800 cm^{-1} = 28 mmol BeB_2D_8/Ar = 1/300 deposited in 3.5 hr; lower trace below 800 cm^{-1} = 53 mmol BeB_2D_8/Ar = 1/300 deposited in 6.5 hr. B, Raman spectrum (14°K), 35 mmol BeB_2D_8/Ar = 1/150 deposited in 18 hr; 500 mW 4880 at sample, 5 cm^{-1} S.B.W.

(e) Isolation of one of several structures in equilibrium at room temperature. This postulate is favored since it is in complete accord with the matrix results and, as outlined below, is also consistent with a number of other observations on the vapor.

Other Evidence for Two Coexisting Structures. Barring the unlikely possibility of massive contamination in the different electron diffraction experiments, a two structure hypothesis seems to offer the only reasonable explanation of the varying diffraction results. That there is rapid tautomeric exchange among the terminal and bridging hydrogens of most borohydrides (*e.g.*, $Al(BH_4)_3$, $Zr(BH_4)_4$, and $Hf(BH_4)_4$) has been clearly shown by proton and ^{11}B nmr studies.[22] Such a reorientation process very likely occurs for BeB_2H_8 also[22] and it is quite conceivable that an equilibrium might

(22) B. D. James, R. K. Nanda, and M. G. H. Wallbridge, *J. Chem. Soc. A*, 182 (1966).

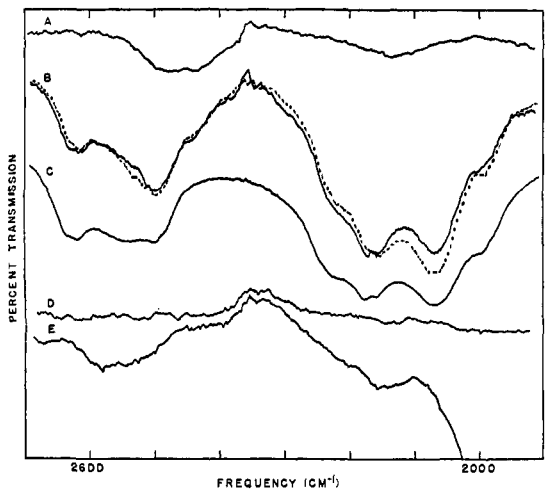

Figure 5. Infrared spectra of beryllium borohydride (10-cm LiF cell): A, background, empty cell after evacuation of BeB_2H_8 10×; B, effect of temperature, 2-mm BeB_2H_8 10× (—) $T = 35°$, (-----) $T = 60°$; C, effect of pressure, 16-mm BeB_2H_8 (saturated vapor at 35°) 1×; D, background, empty cell after evacuation of BeB_2D_8 10×; E, BeB_2D_7H in 6-mm BeB_2D_8 10×.

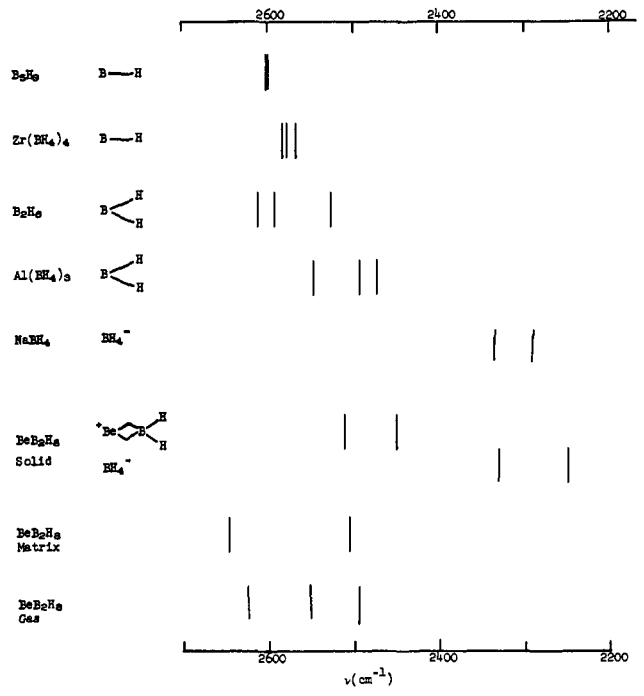

Figure 6. Terminal BH stretching frequencies.

exist between low energy "triangular" and "linear" forms. Under the nonequilibrium conditions of the electron diffraction experiment, it is possible that one or the other form might predominate depending upon the pressure, temperature, and sampling conditions. To test this hypothesis, we have examined the effect of temperature and pressure on the infrared spectrum of the equilibrium vapor.

The effect of pressure is indicated in Figure 5 by the solid traces B ($P \sim 2$ mm, 10× expansion) and C ($P \sim 16$ mm, saturated vapor, 1× expansion). Both spectra are at 35° and, when one takes account of the relative contribution of the window (LiF) absorptions (A, ×10 expansion) in the low pressure spectrum, there appears to be no marked pressure dependence. Addition of 1 atm of argon or nitrogen also has no effect. This is in accord with the absence of dimers shown by the vapor density measurements but is at variance with Cook and Morgans' observations[14] using BaF_2 windows. However, we have not been successful in duplicating their work using BaF_2, LiF, or CsI windows and feel that their spectra include absorptions due to impurities and/or window absorptions. Alternatively, this discrepancy might be cited as further evidence for several forms of BeB_2H_8 although it is difficult to understand such a difference for the equilibrium situation which must apply in the infrared experiment.

The effect of temperature on the spectrum at low pressure (~2 mm) is shown in Figure 5B. A small but reversible and reproducible effect is noted which exactly parallels the dramatic intensity changes on "cooling" the vapor to 20°K *via* the matrix. Similar results are obtained at higher pressure. Although such changes might be due to intensity shifts among P, Q, and R branches, we reject this possibility because of the earlier arguments for assignment of all features as unresolved PQR envelopes.[23] Though small, the temperature effect on the vapor equilibrium is consistent with a two structure hypothesis. Further support comes from the vapor Raman spectrum in which one sees two (or three) polarized terminal BH stretching modes and three (or four) polarized bridge stretches, all above 2000 cm^{-1}. If these are all fundamentals, only model X (three of each predicted) of structures I–X is acceptable. However, in view of the low detectability in the Raman experiment at these pressures, it would be surprising to observe all of these modes. Moreover, the very low depolarization ratios of almost all polarized features above 2000 cm^{-1} seems most consistent with two (or more) molecules. From the infrared and Raman intensities, roughly comparable amounts of the two forms must be present in the equilibrium vapor. Possibly this ratio may change in the diffraction experiments depending on the temperature and sampling conditions but the spectroscopic studies cannot prove this. In any event, it seems clear that any single structure deduced for the vapor from either the diffraction or spectroscopic observations is subject to question. Since the matrix spectrum suggests that predominantly one of the two forms is trapped, its interpretation offers the best hope of deducing both structures.

Structure in the Matrix. Although the interpretation of the matrix spectrum is complicated by the possibility of two molecular species and by the possible observation of combinations or overtones, the large number of infrared (29) and Raman (21) features seems most consistent with a structure of relatively low symmetry. In particular, models I (D_{3d}) and II (D_{2d}) would not be favored. A *definitive* elimination of any of the other eight models on the basis of the number, position, and polarization behavior of the vibrational peaks is not possible because of the aforementioned complications, because of the large frequency uncertainty for the broad overlapping bands, and because of the low sensitivity in the Raman experiments. However,

(23) A possible exception might be the doublet at 2176 and 2158 cm^{-1}. These could be Q (2175 cm^{-1} in the Raman) and P branches of a parallel mode, but, in view of the overlap with adjacent fundamentals, it seems dangerous to draw any structural inferences from this separation.

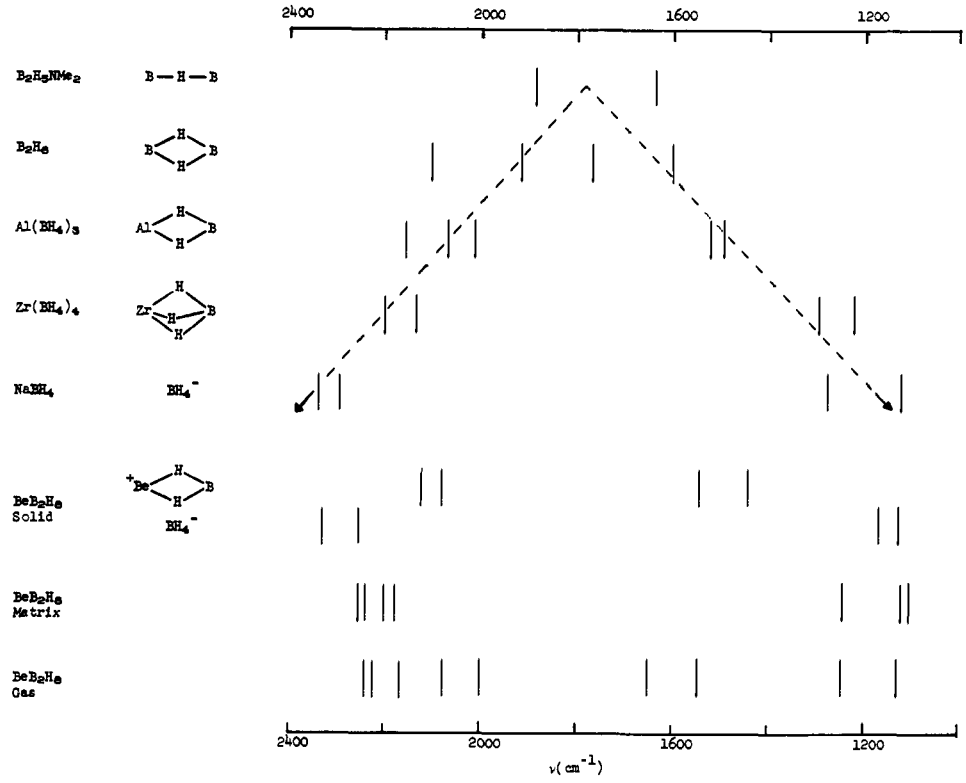

Figure 7. Bridge BH stretching frequencies.

comparison of the stretching frequencies with those of the borohydrides which have been studied in detail[13,16,22-26] does point toward a unique structure.

Figures 6 and 7 are useful in characterizing these BH stretching frequencies. Figure 6 illustrates the decrease in the average terminal stretching frequency as one goes from terminal BH to BH_2 to BH_4^-. The bond lengths tend to increase ($Zr(BH_4)_4$, 1.18 Å;[27] B_2H_6, 1.196 Å;[28] $Al(BH_4)_3$, 1.196 Å;[29] and $NaBH_4$, 1.255 Å[30]), reflecting the weakening of the terminal bond as the electrons are shared among more two-center terminal bonds. Figure 7 shows that the bridge stretches also change in a systematic and pronounced manner as one goes from BHB to MH_2B to BH_4^-. As indicated by the dashed arrows, the frequencies tend to split, approaching pure BH stretching and BH_2 bending modes in the limit of ionic BH_4^-. The increase in stretching frequency is accompanied by an expected decrease in the BH_b bond length (B_2H_6, 1.339 Å;[28] $Al(BH_4)_3$, 1.283 Å;[29] $Zr(BH_4)_4$,1.27 Å[27]; $NaBH_4$, 1.255 Å[30]).

The frequencies for solid BeB_2H_8 are plotted on these figures according to their assignment[13] to $^+BeH_2BH_2$, and BH_4^- ions and it is seen that the spectrum fits this interpretation quite nicely. Encouraged by this agreement, we have also plotted frequencies for matrix isolated and gaseous BeB_2H_8 and it is apparent that these clearly differ from the solid frequencies.

In the matrix, the very high terminal BH stretch at 2645 cm^{-1} strongly suggests the presence of a *terminal BH group* and this is supported by the bridge frequencies which are characteristic of a *triple MH_3B group*. The absence of any intense features in the MH_2B or MHB bridge-stretching region leads us to propose that, in the matrix, the molecule *must have either the D_{3d} (I) or C_{3v} (IX) structure*. Of these, the "double minimum" C_{3v} structure is decidedly favored since the observation of *two distinct, equally intense triple bridge stretches* at 2248 and 2175 cm^{-1} for BeB_2HD_7 contaminant in BeB_2D_8 (Figure 3a) is compelling evidence that the molecule contains *two different types of triple bridges*. A precedent for a double minimum configuration for Be compounds exists in $Be(C_5H_5)_2$[31] and, in view of the structure of solid BeB_2H_8, octahedral coordination around the Be atom is no longer anomalous.

We have also searched for two distinct terminal BH stretches in BeB_2HD_7 but have only been able to clearly detect one very weak feature at 2623 cm^{-1} (Figure 3A). This may be due to the low concentration (H/D estimated at 2%) and the low inherent intensity of the terminal stretches compared to the bridge stretches (substitution at the bridge positions is also three times as probably as at the terminal positions). Alternatively, the two stretches may coincide because of the small coupling between them. In any event, the near proximity of 2623 cm^{-1} to the 2645 cm^{-1} band of BeB_2H_8 (*vs.* the 2565 and 2505 cm^{-1} bands) is most consistent with a terminal BH group rather than the uncoupling of a BH_2 group on partial deuteration (*e.g.*, the terminal

(24) (a) R. C. Lord and C. Nielsen, *J. Chem. Phys.*, **19**, 1 (1951); (b) A. R. Emery and R. C. Taylor, *Spectrochim. Acta*, **16**, 1455 (1960).
(25) H. J. Hrostowski and G. C. Pimentel, *J. Amer. Chem. Soc.*, **76**, 998 (1954).
(26) D. E. Mann, *J. Chem. Phys.*, **22**, 70 (1954).
(27) V. Plato and K. Hedberg, *Inorg. Chem.*, **10**, 590 (1971).
(28) L. S. Bartell and B. L. Carroll, *J. Chem. Phys.*, **42**, 1135 (1965).
(29) A. Almenningen, G. Gundersen, and A. Haaland, *Acta Chem. Scand.*, **22**, 328 (1968).
(30) P. T. Ford and R. E. Richards, *Discuss. Faraday Soc.*, **19**, 230 (1955).
(31) A. Almenningen, O. Bastiansen, and A. Haaland, *J. Chem. Phys.*, **40**, 3434 (1964).

Table IV. Molecular Vibrations of Beryllium Borohydride, C_{3v} Model IX

	BeB_2H_8				BeB_2D_8				
	Gas		Argon matrix		Gas		Argon matrix		
	Ir	Raman	Ir	Raman	Ir	Raman	Ir	Raman	ν_H/ν_D
A_1 vibrations (ir, R, p)									
ν_1(u)[a] νBH_t, asym	2624 m		2645 m		2000 w		2003 w		1.32
ν_2(g) νBH_t, sym		2627 m, p		2643 s, p					
ν_3(g) νBH_b, sym, in phase		2240 m, p		2255 s, p			1595 w, sh	1597 m, sh, p	1.41
ν_4(u) νBH_b, sym, out of phase	2167 s	2175 s, p	2172 m	2179 s, p	~1580 s, b	1578 s, p	1577 vs	1583 s, p	1.38
ν_5(u) δBH_{3b}, sym, out of phase	1130 w		1123 m					1033 w, p	1.09
ν_6(g) δBH_{3b}, sym, in phase		~1150 vw, b		1105 s, p, ?				1002 m, p	1.10
ν_7(u) νBBeB, asym	~1050 vs, b		1051 vs		895 vs		893 vs		1.18
ν_8(g) νBBeB, sym		535 s, p		540 m, p		478 s, p		471 w	1.13
A_2 vibrations (inactive)									
ν_9(u) torsion									
E vibrations (ir, R)									
ν_{10}(g) νBH_b, asym, in phase	2225 m, sh		2241 s	2235 w, sh				1617 m, dp, ?	1.38
ν_{11}(u) νBH_b, asym, out of phase			2202 vs		1650 m, sh		1647 vs		1.34
ν_{12}(u) δBH_t, asym				1298 w, dp				940 vw	1.38
ν_{13}(g) δBH_t, sym			1284 w				928 vw, sh		1.38
ν_{14}(u) δBH_{3b}, asym, out of phase	1247 w		1245 s		1075 w		1074 s		1.16
ν_{15}(g) δBH_{3b}, asym, in phase			1184 vvw	1184 vw					
ν_{16}(g) bridge bend, sym			386 vw	390 vw, dp			322 m		1.20
ν_{17}(u) bridge bend, asym			368 vw				302 m		1.22
ν_{18}(u) BBeB bend	287 w		280 vs	290 vw, dp	275 m		253 vs	261 vw, dp	1.10

[a] Inversion symmetry under D_{3d} symmetry, g = Raman active, u = infrared active.

BH stretch of B_2HD_5 occurs at 2565 cm^{-1}, midway between the B_2H_6 vibrations at 2612, 2591, 2525, and 2524 cm^{-1}). The fact that the infrared peak at 2645 cm^{-1} is accompanied by a polarized band at 2643 cm^{-1} in the Raman also favors a BH group since the polarized symmetric stretch of a BH_2 group is generally significantly lower than the asymmetric stretch (by ~76 cm^{-1} for B_2H_6, ~66 cm^{-1} for $Al(BH_4)_3$, and 59 cm^{-1} for solid BeB_2H_8).

Thus both the characteristic frequencies and the isotopic data indicate a C_{3v} model for the matrix isolated molecule. Further support for this postulate comes from the detailed frequency assignment given below since it is seen that a reasonable assignment of the spectrum is possible for this structure.

Frequency Assignment for C_{3v} Model IX. Table IV summarizes the frequency assignments for the vibrations of C_{3v} model IX. The D_{3d} inversion behavior is also indicated by the g or u label and is useful in the frequency assignments since, if the distortion from D_{3d} symmetry is small, the Raman and infrared intensities should tend toward mutual exclusion behavior. It should be stressed that the mode descriptions are only approximate and, for example, the BH_{3b} bends could equally well be described as BeH_b stretches. In the following discussion, matrix frequencies will be cited where possible (because of their lower frequency uncertainty) and BeB_2D_8 frequencies will be given in parentheses.

The strong infrared feature at 2645 (2003) cm^{-1} is assigned as the asymmetric stretch ν_1. Only slight coupling would be expected between these remote terminal bonds and hence the polarized Raman band at 2643 cm^{-1} is assigned as ν_2, the symmetric stretch. The near identity of these frequencies is consistent with the observation of only one terminal BH stretch (2623 cm^{-1}) for BeB_2HD_7 and with the relative insensitivity of the terminal BH frequencies to variations in bridge bonding (contrast Figure 6 with Figure 7, note scale change). On this basis, we prefer this assignment to the possible alternative assignments at 2645 and 2505 (1820) cm^{-1}. The latter feature seems more likely to be due to the second form of BeB_2H_8 because of the characteristic loss of intensity upon matrix isolation for its strong, polarized, gas-phase counterpart at 2490 (1826) cm^{-1} in the Raman. Accordingly, the 2505-cm^{-1} feature and the weak peak at 2565 (1925) cm^{-1} are ascribed to the second form of BeB_2H_8. It is worth noting that these frequencies would be appropriate to the symmetric and asymmetric stretch, respectively, of a terminal BH_2 group.

Two strong, polarized (and hence A_1) Raman bands are observed at 2255 (1597) and 2179 (1583) cm^{-1} and these are assigned as ν_3 and ν_4. The latter is chosen as ν_4 because it is also intense in the infrared. The close proximity to the BeB_2HD_7 features at 2248 and 2175 cm^{-1} suggests that there is only slight coupling between the "internal vibrations" of the two BH_4 groups and that the asymmetric stretches ν_{10} and ν_{11} will be near ν_3 and ν_4, respectively. ν_{11} should be more intense than ν_{10} in the infrared and hence the strong features at 2202 (1647) and 2241 (1617) cm^{-1} are assigned respectively. The correspondence of the 2202- and 1647-cm^{-1} peaks is established by their absence in the Raman matrix spectrum. The 1617-cm^{-1} Raman feature is only assigned tentatively as ν_{10} for BeB_2D_8 because its intensity behavior suggests the possible contribution of a second species. With these assignments, the H/D ratios for the symmetric (and in phase) stretches are slightly higher than for the asymmetric (and out of phase) stretches, as would be expected.

The broad and intense infrared band at 1050 (895) cm^{-1} is assigned as ν_7, the asymmetric BBeB stretch. Since this mode leads to $BH_4^- \cdots {}^+BeBH_4$ in the limit,

it can be expected to give rise to a large dipole derivative and, indeed, the 1050- and 895-cm^{-1} features are the most intense infrared features. Similarly, very high intensity is observed for the corresponding stretches in $Al(BH_4)_3$ (602 cm^{-1}), $Zr(BH_4)_4$ (509 cm^{-1}), and solid $^+BeBH_4$ (725 cm^{-1}). (The infrared inactive stretch for B_2H_6 occurs at 794 cm^{-1}.) In view of the light Be mass and the triple hydrogen bridge (*vs.* a double bridge for solid $^+BeBH_4$), 1050 cm^{-1} seems a reasonable value and, in any event, the absence of any strong infrared feature from 300 to 1050 seems to require the assignment. The H/D ratio of 1.18 is relatively high, indicating substantial mixing with the nearby BH_{3b} bends.

By analogy with $Al(BH_4)_3$, the symmetric BBeB stretch, ν_8, should be lower in frequency and should be reasonably intense in the Raman but weak in the infrared. The strong, polarized gas-phase Raman peak at 535 (478) cm^{-1} shows the appropriate behavior although the reduced Raman intensity and complex structure of this band in the matrix suggests that the second form of BeB_2H_8 may also contribute in this region. (Examination of both the 500- and 1100-cm^{-1} regions in the Raman matrix spectra of Figure 3B and 3C shows anomalous intensity variations which are thought to be due to varying amounts of the second form or to trapped $BeBH_5$ and/or BeH_2 polymer.) That ν_7 and ν_8 should be split so much (for $Al(BH_4)_3$ the splitting is 602 − 510 = 92 cm^{-1}) is perhaps not too surprising since these modes most directly sample the unusual force field about the Be atom. Movement of one BH_4 unit relative to the Be atom should profoundly influence its bonding to the other BH_4 group and hence the coupling will be unusually large. Analogous coupling occurs for multiple bond compounds such as CO_2 (symmetric stretch, 1388 cm^{-1}; asymmetric stretch 2349 cm^{-1}).

The BBeB bend, ν_{18}, must clearly be assigned at 280 (253) cm^{-1} because of the low frequency and the relatively small isotope effect (H/D = 1.10). The corresponding in plane bend for $Al(BH_4)_3$ occurs at 318 (267, H/D = 1.19) cm^{-1}. The lower value for this mode in BeB_2H_8 (despite the lighter Be mass compared to Al) is understandable in terms of the reduced role of directional covalent bonding in the Be compound. The other expected low frequency modes, the bridge bends ν_{16} and ν_{17}, we assign as the 386 (322) and 368 (302) cm^{-1} features. Their relatively low H/D ratios of 1.20 and 1.22 are reasonable since these modes will mix heavily with ν_{18}.

Assignment of the remaining vibrations is more difficult. Terminal BH bending frequencies have been assigned at 1620–1440 cm^{-1} in B_5H_9[25] but Bellamy, *et al.*,[32] have suggested that the region 1075–1010 cm^{-1} is more appropriate. For $Zr(BH_4)_4$ and $Hf(BH_4)_4$ (both presumed to have triple bridges) a weak band appears at 1295 and 1300 cm^{-1}, respectively.[22] Since the bending mode should be relatively weak and only slightly shifted in going from Zr to Hf (and perhaps to Be) we assign the weak infrared feature at 1284 (928) cm^{-1} and the weak, depolarized Raman band at 1298 (940) cm^{-1} as ν_{13} and ν_{12}, respectively. The closeness of these frequencies is consistent with the small coupling between the well-isolated BH bonds.

The four BH_{3b} bends ν_5, ν_6, ν_{14}, and ν_{15} are expected in the 1250–1000-cm^{-1} region by analogy with bands in $Zr(BH_4)_4$ at 1223 bs, 1165, vw, and 1040 vw and in $Hf(BH_4)_4$ at 1228 vs, 1140 vw, and 1020 vw. Tentative assignments are given for these which seem most consistent with the observed infrared and Raman intensities but alternate assignments might be possible.

From the above it is clear that an acceptable assignment of all the strong infrared and Raman matrix features is possible in terms of a C_{3v} model. The weaker matrix features which correlate with the more intense gas-phase bands at 2550, 2500, 2071, 2000, 1650, 1548, 1000, and 588 cm^{-1} are surely due to a second form of BeB_2H_8. These frequencies suggest the presence of terminal BH_2 and bridging BH_{2b} groups and could reasonably be assigned to the classical D_{2d} structure II. However, an equally acceptable assignment in terms of a bent structure such as III–V also seems possible. Efforts to resolve this by examination of the BH stretches of BeB_2HD_7 vapor (Figure 5E) have not been helpful and hence we do not feel a conclusion as to the second structure of BeB_2H_8 is justified at this time.

On the Bonding in BeB_2H_8. Inasmuch as the matrix data have led to quite a novel structure for BeB_2H_8, some discussion of the unusual bonding about the Be atom is warranted. Most beryllium compounds exhibit tetrahedral coordination and hence the author has had to overcome his initial bias in favor of the classical D_{2d} structure II. With the exception of solid BeB_2H_8, no other case of octahedral coordination about the Be atom has been reported. Just as the boron hydrides are not easily represented by simple valence bond formulas, so too is BeB_2H_8 difficult to describe. Any valence bond representation of the C_{3v} model would require a number of resonating structures and should include a significant contribution by ionic structures such as BH_4^-–Be^{2+}–BH_4^- and BH_4^-–$^+BeBH_4$. Since the molecule is distorted in the matrix, the latter structure is apparently important.

Although the large dipole moment (2.1 ± 0.5 D) observed in the gas may arise in part from the second BeB_2H_8 species, the C_{3v} model itself should have a significant dipole moment. If the molecule is viewed as BH_4^-–Be^{2+}–BH_4^-, a displacement of 0.22 Å of the Be atom would yield μ = 2.1 D. From a simple electrostatic calculation using the electron diffraction B···B distance of 3.6 Å, one obtains a central barrier maximum of 3600 cm^{-1} or 10 kcal/mol relative to the 0.22-Å "minima." This value has no quantitative significance of course, but it is of a reasonable magnitude (for example, the inversion barrier for NH_3 is about 2000 cm^{-1}). Because of the mass of the Be atom, tunneling should be slow and no detectible vibrational splitting would be expected.

Of course, the complete charge separation implied by BH_4^-–Be^{2+}–BH_4^- is unrealistic and unnecessary. If one views the molecule as $BH_4^{-\delta}$–$^{+\delta}BeBH_4$, a value of δ of only about 0.25 e^- would be sufficient to produce a dipole moment of 2.1 D. Whichever description is more correct, it is clear that the situation is quite analogous to that in $(C_5H_5)_2Be$. In this molecule, the Be is displaced 0.25 Å toward one ring[31] and a substantial dipole moment is observed: 2.46 ± 0.06 D in benzene and 2.24 ± 0.09 D in cyclohexane.[33] Thus

(32) L. J. Bellamy, W. Gerrard, M. F. Lappert, and R. L. Williams, *J. Chem. Soc.*, 2412 (1968).

(33) E. O. Fischer and H. P. Hofmann, *Chem. Ber.*, **92**, 482 (1959).

for both molecules, electrostatic forces must play an important role in the bonding.

The molecular structure can also be understood in terms of molecular orbitals. By a straightforward application of group theory, it is easy to construct 20 symmetrized molecular orbitals using as a basis set the 8 hydrogen 1s orbtials and the 12 beryllium and boron 2s and 2p orbitals. From an examination of the nodal planes of the orbitals of a D_{3d} model, one would expect six bonding orbitals ($2A_{1g} + 2A_{2u} + E_g + E_u$), three nonbonding orbitals ($A_{1g} + A_{2u} + E_u$), and six antibonding orbitals ($2A_{1g} + 2A_{2u} + E_g + E_u$). Distortion to a C_{3v} structure will only result in a slight mixing of the A_{1g} and A_{2u} functions and of the E_g and E_u functions. The six bonding orbitals can just accommodate the 16 available electrons and the electronic configuration for the $^1A_{1g}$ ground state can be written $(1A_{1g})^2(1A_{2u})^2(2A_{1g})^2(2A_{2u})^2(1E_u)^4(1E_g)^4$. The first two orbitals essentially localize four electrons in the terminal BH bonds and the remaining 12 electrons are distributed in the bridging regions. In the absence of the bridging protons, the electron density distribution would be cylindrically symmetric but addition of the protons so as to minimize electrostatic repulsions would give a D_{3d} configuration. It seems likely that the resistance to torsion would be small and thus the inactive torsional frequency, ν_9, is apt to be quite low. It is noteworthy that the electronic configuration is quite analogous to that of the isoelectronic molecule CO_2 [$^1\Sigma_g^+ = (3\sigma_g)^2(2\sigma_u)^2(4\sigma_g)^2(3\sigma_u)^2(1\pi_u)^4(1\pi_g)^4$] and thus the comparable coupling of the symmetric and asymmetric stretches noted earlier for the two molecules is understandable. Similarly, no electronic transitions would be expected in the visible region for BeB_2H_8, a prediction supported by the transparency of the vapor down to 1900 Å.

Acknowledgment. Acknowledgment is made to the donors of the Petroleum Research Fund, administered by the American Chemical Society, for support of this research. National Science Foundation (Grant GP 24608) and Research Corporation support for the development of Raman matrix isolation techniques is also acknowledged. In addition, we are grateful for a National Science Foundation contribution toward the purchase of the Cary 82 Raman spectrometer (Departmental Development Award) and the Perkin-Elmer 180 infrared spectrophotometer (Departmental Equipment Grant) used in this work. Finally, the author wishes to thank Professors J. W. Linnett and H. J. Emeléus for their kind assistance in some of the preliminary work initiated on this project during a postdoctoral year at the University of Cambridge.

Chemical Ionization Mass Spectrometry. XVIII. Effect of Acid Identity on Decomposition Rates of Protonated Tertiary Alkyl Esters

W. A. Laurie and F. H. Field*

Contribution from Rockefeller University, New York, New York 10021.
Received November 12, 1971

Abstract: Kinetic studies were made using the chemical ionization technique of the decompositions of four esters: *tert*-amyl *n*-propionate and *tert*-amyl *n*-butyrate using isobutane as reactant gas and *tert*-butyl *n*-propionate and *tert*-butyl *n*-butyrate using isopentane as reactant gas. It is found that the rates of decomposition are independent of the chain length of the acid portion of the ester. This is in contrast to the effect found previously of the length of complexity of the chain in the alcohol portion of the ester. As a further illustration of this effect, the rate of decomposition of gaseous protonated 3-ethyl-3-pentyl acetate was found to be faster than any acetate investigated so far.

We have recently reported[1] the results of a study of the decomposition kinetics of seven gaseous protonated tertiary alkyl acetates. The rates of decomposition of the protonated molecule ions to the tertiary alkyl ions and acetic acid were measured, and a good correlation with structure was obtained. In brief, as the size and complexity of the alkyl groups increased the rates of decomposition increased. In this study we have investigated the importance of the identity of the acidic function in the reaction. The compounds studied were *tert*-amyl *n*-propionate and *n*-butyrate using isobutane as reactant gas, and *tert*-butyl *n*-propionate and *n*-butyrate using isopentane as the reactant gas. Synthetic difficulties limited the extension of the study to acids with longer chains. 3-Ethyl-3-pentyl acetate was also measured, which provides a further link with the previous work.

Experimental Section

The experiments were carried out on the Esso Chemical Physics mass spectrometer which has been described elsewhere.[1-6] The

(1) W. A. Laurie and F. H. Field, *J. Amer. Chem. Soc.*, **94**, 2913 (1972).

(2) F. H. Field, *J. Amer. Chem. Soc.*, **91**, 2827 (1969).
(3) F. H. Field, *ibid.*, **91**, 6334 (1969).
(4) D. P. Weeks and F. H. Field, *ibid.*, **92**, 1600 (1970).
(5) F. H. Field and D. P. Weeks, *ibid.*, **92**, 6521 (1970).
(6) (a) M. S. B. Munson and F. H. Field, *ibid.*, **88**, 2621 (1966); (b) F. H. Field, *ibid.*, **83**, 1523 (1961).